京都大学防災研究所年報 第 64 号 B
DPRI Annuals, No. 64 B, 2021

Analysis of Cell Merging from New Cells to Multicell Formation with Dual Doppler and Vorticity Analysis

Fauziana AHMAD (1), Kosei YAMAGUCHI and Eiichi NAKAKITA

(1) Graduate School of Engineering, Kyoto University

Synopsis

The investigation of merging cells from new cells to multicell in thunderstorms using vertical vorticity analysis will be proposed. The vertical vorticity analysis using pseudo-vorticity that used only one single radar and Dual Doppler analysis (DDA) vorticity were applied to the rainfall event on 10th September 2014 with the condition of an unstable atmospheric environment with the weak vertical shear. The core pair vorticity was identified by selecting the maximum quantitative vorticity intensity at each boundary of the new cell and multicell. The comparison of time series core pair vorticity was established before, during, and after the merging cells. It was found that at the early stage of merging cells, new cell B indicated the largest intensity with cell A (older cell), whereas other new cells showed lower strength compared with the multicell after the later stage of multicell formation. This signature pattern was identical for the pseudo-vorticity and DDA vorticity analysis. By employing vertical velocity analysis, the core of the updraft was located between the pair of vorticities which influenced the construction of vertical vortex tubes with the existence of weak wind shear. The supportive mechanism that resulting in the intensification of core pair vorticity was established by examining the convergence, stretching, and tilting of the vortex tube. The convergence plays the main role in the intensification of core vorticity which influenced the stretched of vortex tube to rotate rapidly that generated the increment of core vorticity, meanwhile tilting was less affected to this increment pattern. In conclusion, the signature pattern of merging cells could be observed on the strength of core pair vorticity during the merging cells.

Keywords: new cell, multicell, core pair vorticity, merging cell, updraft, convergence

1. Introduction

The disaster occurrences mainly such as floods and landslides are induced by the severe thunderstorms that generated from the rain cloud. The single cell typically has its lifetime of about one hour and the area of occurrence is basically in the small area. However, the multicell could also produce the higher intensity of precipitation which contributes to severe disaster due to its lifetime of more than an hour and the scale of areas are larger than a single cell.

The weather pattern could be observed by the weather radar because of its better temporal and spatial resolution and Doppler radar is capable to estimate precipitation amounts and movement of the precipitation systems (Min Jang, et al., 2014). A single Doppler radar measures one component of the wind vector which is moved towards or away from the radar that is stated as radial wind. With a Dual Doppler radar, the three-dimensional wind vectors with two-dimensional horizontal wind and vertical

wind could be retrieved. We can measure two components of the wind by assuming the vertical component of the wind is small (Ronald E., 2004). Therefore, Dual Doppler analysis is established to analyze the multicell formation using vorticity and the additional factors that might be influenced the development of the rotation.

Vorticity analysis in the single cell was investigated and it was found that vorticity could be useful in the detection of Guerilla-heavy rainfall before the development of the cumulus stage (Nakakita, E., et al., 2017). Meanwhile, the heavy precipitation from the supercell was well-understood which the existence of vertical vorticity supported via tilting of horizontal vorticity associated with the vertical shear of environmental wind profile (Markowski, et al., 2010). The multicell formation using the vorticity analysis technique was established and the signature pattern of merging from the single cell to multicell was difficult to examine due to change of core vorticity at upper-level height (Ahmad, et al., 2020). However, other criteria were suggested to identify the pattern of core vorticity by focusing on the strength of core vorticity in each boundary of cells.

Therefore, the objectives of this study are to further investigate the signature pattern of the multicell formation using vorticity analysis by applying the pseudo-vorticity and Dual Doppler techniques and clarify the mechanism that influences the multicell formation.

2. Data and Methodology

In this section, we will discuss the methodology for the cell classification with the merging echoes and vorticity extraction from two methods namely pseudo-vorticity and Dual Doppler Analysis (hereafter referred to as DDA).

2.1 Cell Merging

The multicell thunderstorms consisted of two or more cells that divided into new cells, mature cells, and older cells at various stages. Commonly, its lifetime is more than one hour, and the scale area are larger than a single cell. New cells usually developed on the western or southwestern edge of the storm constantly in the developing stage. Meanwhile, the

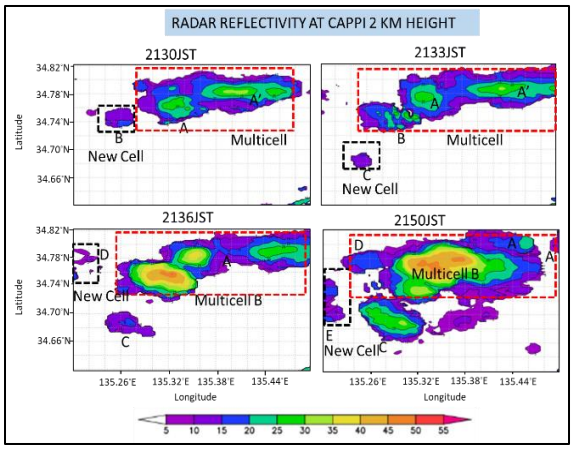

Fig. 1 The classification of new cell and multicell for nearly one-hour observation at the target area.

older cell located at the east or northeast of the storm is always in the dissipating stage. In this study, a new cell is defined as a cell that is developed near the storm which the range less than 20 km from the center of the storm, and a multicell is the cell is merged with one or more of the new cell and its lifetime more than one hour. The classification of the cell naming is recognized according to the appearance of cell starting from A, B, C in the formation order with the closed contour of radar reflectivity (Z_h) greater than 10 dBZ existed at 2 km height as shown in Fig.1. In the meantime, the merging of echoes between new cell and multicell is defined by observing the edge of the contour line of echoes more than 10 dBZ at 2 km height and observed the increasing of Z_h after five minutes merging as presented in Fig.2.

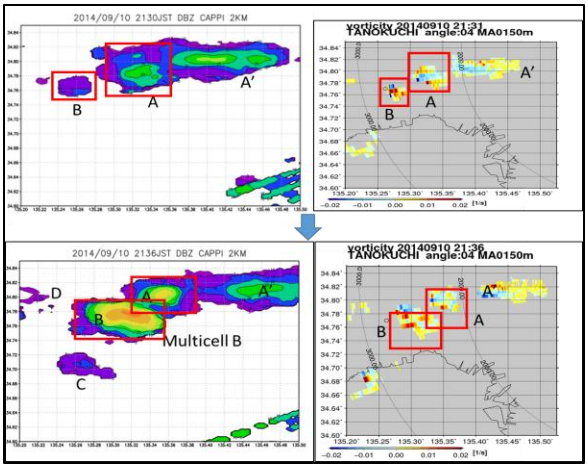

Fig. 2 Boundary of cell merging (red color box) between new cell B and older cell A.

2.2 Pseudo-Vorticity Analysis

In the vorticity analysis, the X-band Multi-Parameter Radar Observation extended radar information network (XRAIN) that operated by the Ministry of Land, Infrastructure, Transport, and Tourism (MLIT), Japan used for this study. The selection of radar stations is depended on the distance from the target area. Tanokuchi radar station will be used in the pseudo-vorticity analysis. This radar performed one volume scan observation in 5 minutes with a maximum range is 80 km. However, to obtain the precise vorticity distribution, the methodology adapted from (Nakakita, E., et al., 2017), the raw data in the polar coordinate system was directly used by converting Plan Position Indicator (PPI) into a two-dimensional Cartesian coordinate system. For the extraction of pseudo-vorticity distribution, equation (1) was used by utilizing Doppler weather radar estimation which the temporal and spatial resolution were one-minute and 50m x 50m respectively for each PPI image at a moving average of 150m.

$$\xi = 2 \times \frac{v_a - v_b}{2r} \qquad (1)$$

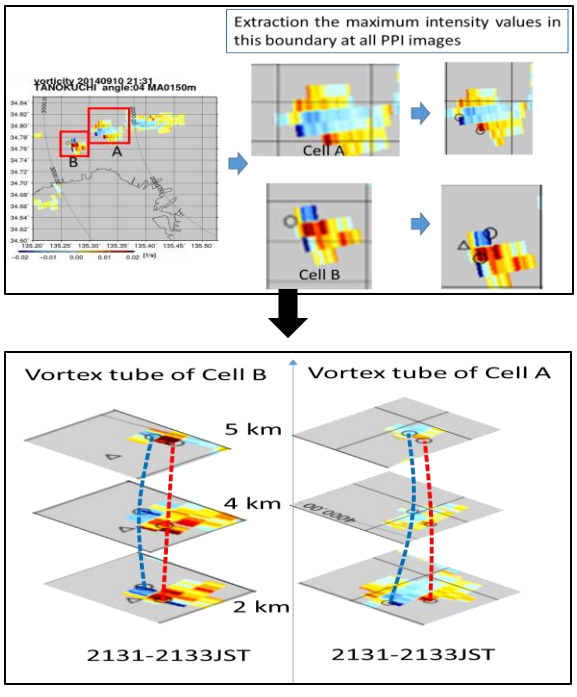

Fig. 3 The construction of vortex tube from the core pair vorticity distribution.

For this study, we would like to examine the core pair vorticity which is defined as the maximum intensity values at each time observation during the period of analysis for cell boundary for positive and negative vorticity. The location of core pair vorticity should be indicated the continuity of the vortex tube construction as illustrated in Fig. 3.

2.3 Dual Doppler Analysis

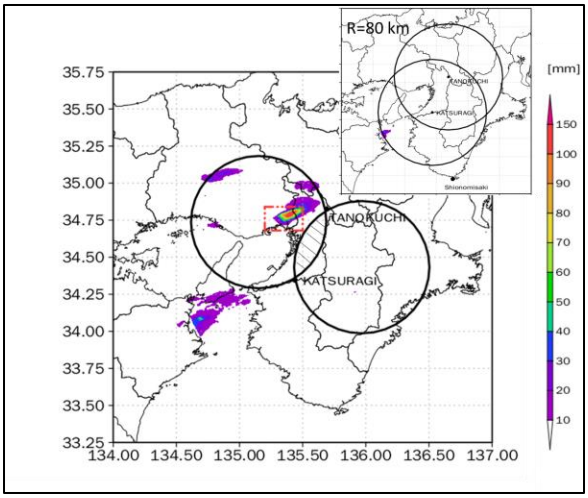

Fig. 4 Two Doppler radars at Tanokuchi and Katsuragi cover a radius of 80 km (the full observation domain is shown in a box at the upper-right corner. Dual Doppler radar map used for the target area (red box color) was conducted within two solid circles except for the hatched area. The accumulated rainfall from 2100 until 2330JST is shown in this image.

Tanokuchi and Katsuragi radar stations will be deployed in the Dual Doppler Analysis (DDA) will be used two radar stations as shown in Fig. 4. Both radars performed one volume scan observation in 5 minutes with a maximum range is 80 km. We conducted a Dual-Doppler analysis using the variation method proposed by (Protat, et al., 1999) since its advantage on the detection of updraft from the lower level with the boundary conditions of w =0 ms^{-1} at ground level and the storm top were employed. Three components of wind (u, v, and w) were retrieved in the Cartesian coordinate system within two solid circles except for the hatched areas in Fig.4 which the intersection angle is less than 30°. The terminal fall velocities of rain, snow and graupel were adapted from (Shimizu, et al., 2008). Spatially and temporally discontinuous and anomalous data were eliminated as noises from Doppler velocities and three-dimensional wind vectors.

The equation (2) is used for the extraction of vorticity distribution by using two Doppler radars with a horizontal grid interval of 0.25 km, and a vertical interval of 0.5 km that were interpolated into a Cartesian coordinate system Constant Altitude Plan Position Indicator (CAPPI) data set.

$$\xi = \frac{\partial v}{\partial x} - \frac{\partial u}{\partial y} \qquad (2)$$

2.4 Supportive Mechanism Analysis

In the development of vertical vorticity within an updraft, the local change of vertical vorticity could be expressed as

$$\frac{\partial \xi}{\partial t} = \zeta \frac{\partial w}{\partial x} + \eta \frac{\partial w}{\partial y} + \xi \frac{\partial w}{\partial z} \quad (3)$$

$$\text{Divergence} = \frac{\partial u}{\partial x} + \frac{\partial v}{\partial y} \quad (4)$$

where (ζ, η, ξ) is the three-dimensional relative vorticity vector, and we have neglected the Coriolis force and baroclinic generation of vertical vorticity, which did not contribute to $\partial\xi/\partial t$ in a major way (Markowski, et al., 2010). The first and second terms of the right-hand side of equation (3) is referred as tilting of horizontal vorticity meanwhile the third term is indicated the stretching of the vortex tube. The convergence is also the vital component that influenced the increment of core vorticity with the stretched vortex tube as referred to in equation (4). The negative of divergence is indicated as convergence in this analysis.

From the study of (Markowski, et al., 2006), the vorticity stretching was the key factor of development at vorticity extrema at the early period of intensification especially near the ground with the existence of convergence at the ground level, whilst tilting also contributed to this impact at the middle boundary layer. In the analysis of (Ohno et. al, 2010), they found that the tilting of horizontal vorticity and stretching of vertical vorticity was the vital supportive role in maintaining or further intensifying the vortices especially with the same sign that closer each the other.

Thus, we would like to analyze the impact factors that influence the core vorticity in the multicell formation related to their intensification and maintenance by investigating the stretching and tilting of vortex tube, convergence, and updraft.

3. Brief description of the atmospheric condition

The selection of study events focused on the broken-areal formation which the lifespan of the multicell formation was 30-90 minutes (Bluestein, H.B., et al., 1985). The target area in this study was observed by Doppler radars for nearly one hour. The multicell storms were observed on the case studies on the 10th September 2014 (2100JST-2200JST) in the Kinki region, Japan.

The radiosonde data from the Shionomisaki station which the distance is about 150 km from the target area was selected. The wind profile was retrieved from Wyoming upper-air observation to calculate Convective Available Potential Energy (CAPE), Bulk Richardson Number (BRN), and the vertical shear from the surface to 6 km. Table 1 showed that the weak vertical shear occurred during these events that appropriated for the multicell formation and not affected by Baiu front or tropical cyclone. Meanwhile, Fig.5 showed the wind hodograph in which a southwesterly wind was predominant up to 11 km above ground level (AGL), with a maximum speed of 15 ms^{-1} at 7.5 km AGL. The multicell formation was favorable in the weak vertical with the existence of warm moist air inflow from the Osaka bay.

Table 1: Parameter observation during the analysis

Parameter	0900JST	2100JST
Vertical Shear	0.003	0.004
CAPE (J/kg)	0	866
BRN	0	60

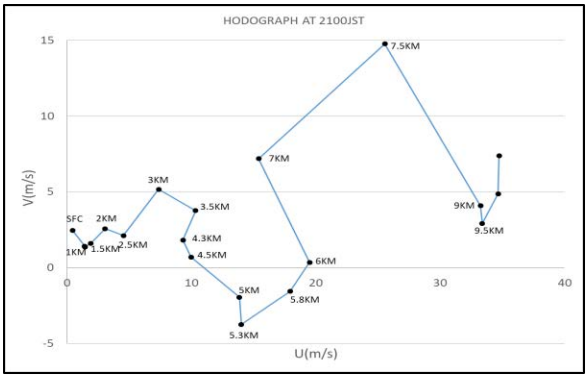

Fig. 5 The hodograph at Shionomisaki station at 2100JST

4. Results and Discussion

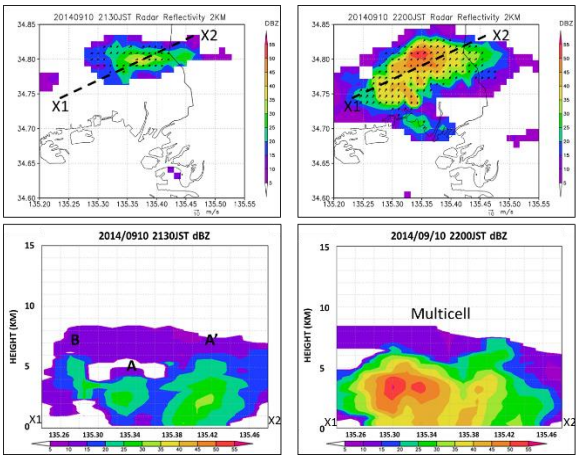

Fig. 6 The cross-section of radar reflectivity throughout the entire storm

In this study, the evolution of multicell formation is presented by Fig. 6 at 2 km height with the information of Z_h and horizontal winds. The storm propagated from southeast to the northeast which started from a single cell and combined with other cells that were newly generated at the left flank of the storm to become multicell. During the one-hour observation, maximum reflectivity was increased from 30 dBZ to 60 dBZ and maximum updraft speed increased from $<1.5ms^{-1}$ to $>3.5ms^{-1}$. The development of multicell formation with the vertical cross-section through the storm will be explained in Section 4.1. The detailed analysis on vorticity in terms of intensity for each cell will be discussed in Section 4.2 and Section 4.3 for pseudo-vorticity and DDA vorticity respectively. The evaluation of the supportive mechanism will be presented in Section 4.4.

4.1 Cell Merging

Table 2: Merging time and pattern for each cell

Cell	Merging Time	Merging Pattern	Distance
B	2134 JST	Fully merged	1.0 km
C	2150 JST	Partial merged	10.8 km
D	2145 JST	Fully merged	0.9 km
E	2152 JST	Fully merged	4.1 km

Table 2 explained about time occurrence of merging time based on the merging criteria stated previously in Section 2.1. We indicated the merging pattern either fully merged or partially merged depends on the merging echoes whether it will separate or not after merging with other cells. From this table, Cell C only showed the partially merged pattern, while the others indicated the fully merged pattern. As stated by (Browning, et al.,1976) the new cell (called daughter clouds) that developed from the parent cell, the distance should be less than 30 km from the core of Z_h. Therefore, we calculated the range from the core of the storm with the new cell and found that the distance for each new cell was less than 10 km.

To understand the mechanism of multicell formation, the vertical cross-section through the storm is presented in Fig.7. We observed that the new convection appeared adjacent to older cells and connected with this parent cell from the left.

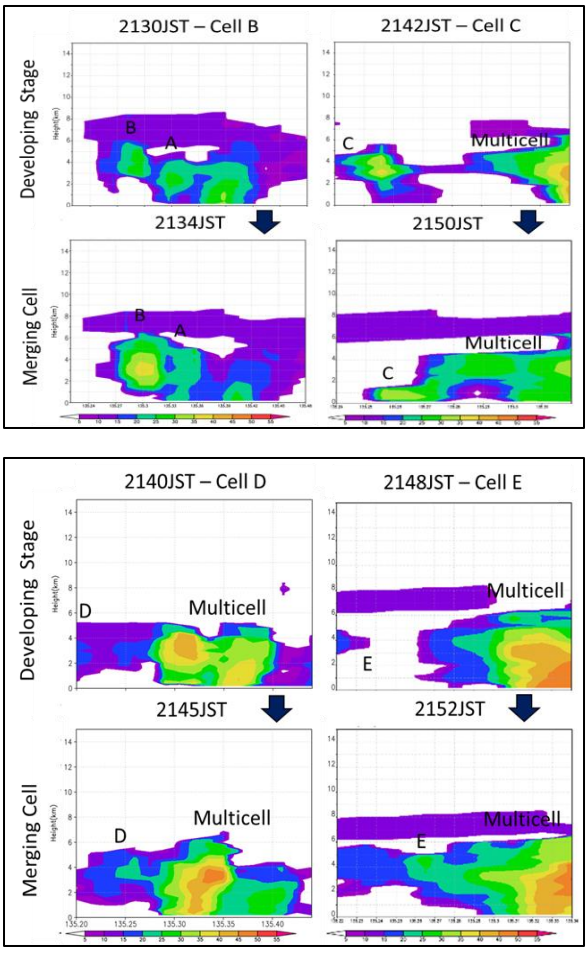

Fig. 7 The vertical cross-section of new cells for Z_h at the developing stage and merging cells

4.2 Pseudo-Vorticity

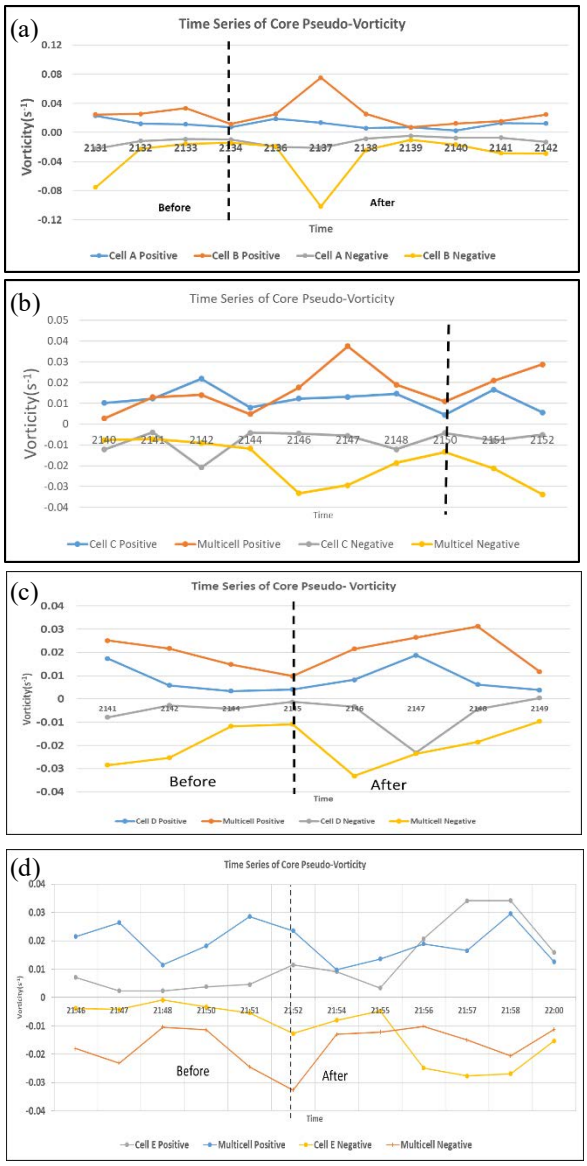

Fig. 8 The pseudo-vorticity between new cell and multicell for positive and negative vorticity, Black dashed line color indicated before and after cell merging.

At the early stage of multicell formation, it was found that new cell B indicated the greatest intensity of vertical vorticity compared with cell A as shown in Fig. 8(a) after the merging occurrence at time 2134JST. Meanwhile, cell C as shown in Fig.8(b) indicated less intensity compared with multicell B during the 10-minute observation. Cell D in Fig. 8(c) showed less intensity during the period for both pair vorticity and cell E as described in Fig. 8(d) indicated the multicell intensity was higher compared with the new cell after the merging.

Consequently, we found that the intensity of core vorticity at the early stage of multicell formation indicated that the new cell showed greater strength with the older cell presented lower intensity of vorticity. Then, multicell revealed a higher intensity of vorticity after merging with other new cells. We observed the peak of core vorticity at each boundary of the cell as summarized in Table 3. The peak core vorticity showed that cell B was the largest value at both pair vorticity followed by the new cell E. Multicell DB and EB indicated almost similar intensity for this period and multicell CB displayed less strength intensity during the analysis.

Table 3: The peak of core pair vorticity for new cell and multicell in pseudo-vorticity analysis

Cell	Intensity (s^{-1})	Multicell	Intensity (s^{-1})
B	0.076 -0.110	A	0.023 -0.020
C	0.022 -0.027	CB	0.019 -0.020
D	0.019 -0.020	DB	0.031 -0.033
E	0.034 -0.028	EB	0.030 -0.033

4.3 DDA Vorticity

We could observe the increment of core vorticity at the early stage of multicell formation from pseudo-vorticity. Since DDA provided the highest quality estimation, we would like to further analyze the vorticity using this method.

From Fig.9, we noticed that the core of updraft was located between the core of vorticity during the merging occurrence at 2135JST. The vorticity of cell B existed at this time and merged with cell A. The updraft showed the highest intensity after merging cell B and cell A with the increment of core vorticity at the boundary area of cell A and cell B. We checked at each CAPPI height and observed that Cell B revealed the largest strength compared with cell A at levels 2.5 km and 3.5 km as presented in Fig. 10. In contrast, the other new cells showed less intensity when they merged with the existing multicell formation during the analysis.

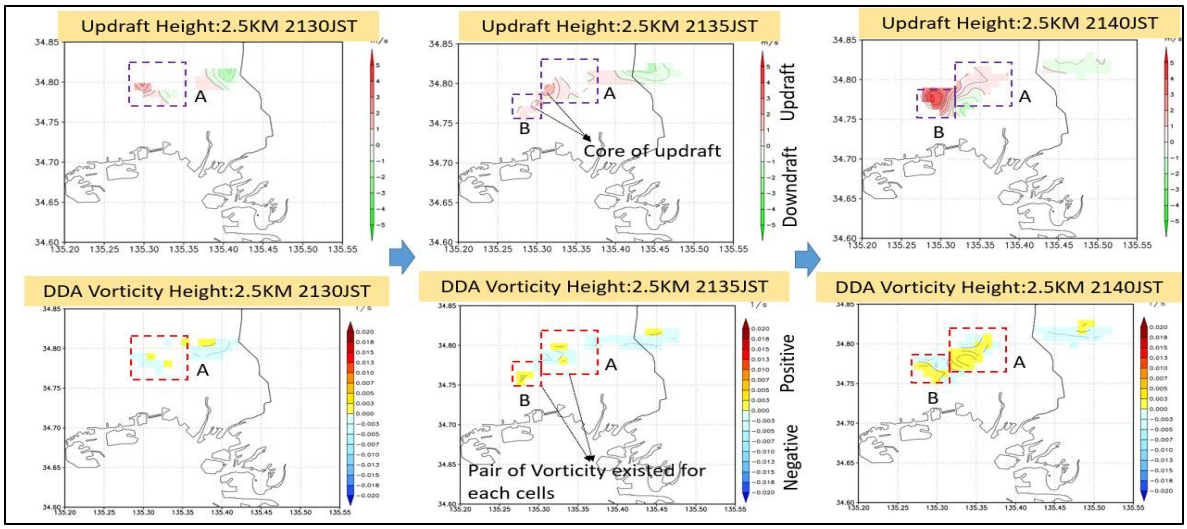

Fig. 9 The one-dimensional image of vertical velocity (top figure) and vorticity (below figure) focused on Cell A and Cell B

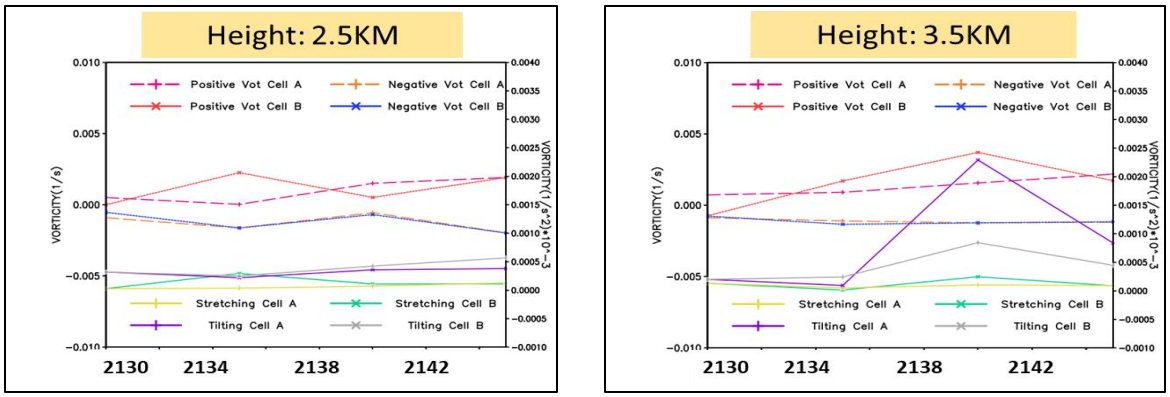

Fig. 10 The line graph of core pair vorticity for cell A and new cell B at height 2.5 km and 3.5 km

We summarize the peak of core vorticity intensity for new cells and multicell as presented in Table 4. We noticed that the multicell formation possessed the persistence of core vorticity intensity during the period of analysis meanwhile, the new cells showed less intensity. We will analyze these persistence results in Section 4.4 and their increment at the early and later stages of multicell formation.

Table 4: The peak of core pair vorticity for new cell and multicell in DDA-vorticity analysis

Cell	Intensity(s^{-1})	Multicell	Intensity(s^{-1})
B	0.005 -0.003	A	0.003 -0.003
C	0.003 -0.002	CB	0.003 -0.003
D	0.002 -0.002	DB	0.003 -0.003
E	0.003 -0.002	EB	0.003 -0.003

4.4 Supportive Mechanism

We studied the supportive mechanism that influenced the increment of core vorticity by analyzing the updraft and convergence mechanism that might contribute to this effect. The study by (Markowski, et al., 2006) found that increment of core vorticity was basically influenced by the local rate change of vertical vorticity at various levels, which stretching of vortex tube commonly occurred at the ground level meanwhile, tilting of vortex tube happened at the middle level. The convergence also provides much more impact to the stretching pattern resulting in the increasing of rotation that yields to the increment of core vorticity intensity.

Thus, these support mechanisms will be evaluated which focused on cell A and cell B as presented in Fig 11. We could observe that the Z_h after merging becomes more intensified with the presence of intense convergence at the boundary of cell B. The strong intensity of tilting of vortex tube indicated that the horizontal vorticity was tilted into

the vertical vortex tube and maintained its intensity whilst, the stretched vortex tube showed intensification at a height of 3 km.

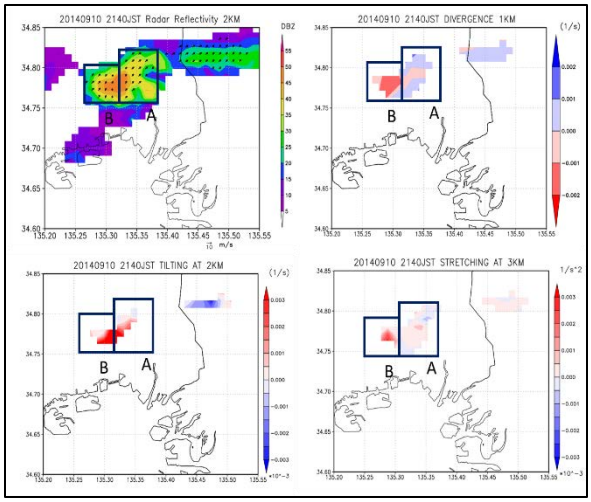

Fig. 11 The horizontal distribution image of supportive mechanism after merging at 2140JST between cell A and cell B

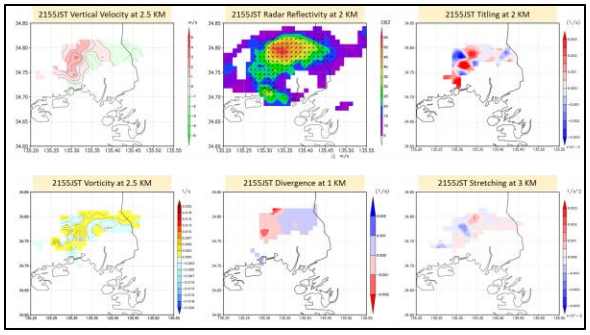

Fig. 12 The horizontal distribution image of supportive mechanism at 2155JST

At the later stage of multicell formation as described in Fig.12, the scale area of multicell formation currently becomes larger and the radar reflectivity and vorticity showed the highest intensity at the center of the storm. The convergence at the lower level at the center of storms indicated the peak intensity with the stretching and tilting strength could be observed at the middle level.

As the analysis revealed that the multicell consisted of the persistence of core vorticity with their values higher than the new cell, we want to investigate the impact from the supportive mechanism. The correlation coefficient between vertical vorticity and the supportive mechanism at cell A, multicell CB, DB, and EB were constructed as presented in Table 5. We found that the updraft and divergence played the main role in the persistence of core vorticity with less effect from the stretching, tilting, and convergence. In the multicell formation, updraft was continuously developed since the new cell was always generated at the left flank of downdraft. The downdraft was associated with the divergence mechanism which the mature cell or dissipating cell always occurred during these stages. The repetition of downdraft and updraft in the multicell formation resulting in the persistence of core pair vorticity with the additional less impact from the stretched and tilted vortex tube that maintained the intensity of core vorticity. The convergence was affected less for this pattern that also contributed to the less effect on the stretching of the vortex tube.

Table 5: The correlation coefficient between supportive mechanism and core vorticity intensity in the persistence analysis

Correlation Coefficient (R^2)	Positive Vorticity	Negative Vorticity
Updraft	0.44	0.03
Divergence	0.36	0.30
Stretching	0.27	0.23
Tilting	0.16	0.00
Convergence	0.00	0.02

5. Conclusions

The signature pattern of cell merging in terms of the intensity of core pair vorticity was established in one-hour period duration utilizing pseudo-vorticity and DDA vorticity analysis. For both analyses, we found that a similar pattern of increment of core vorticity occurred at the early stage of multicell formation that happened at the new cell. Instead, at the later stage of this formation, new cells disclosed the less intense compared with the multicell that consisted of persistence of core pair vorticity intensity. The cell merging could be indicated with the signature pattern of core vorticity strength. The mechanism that supported the increment of core vorticity and the persistence of core vorticity was developed to understand these patterns.

From this study, we discovered that convergence played a key role in the intensification of core pair vorticity along with the stretching of vortex tubes

during the increment of core pair vorticity. Meanwhile, tilting of the vortex tube showed significant intensity to indicate the tilted horizontal vorticity to the intensified of the vertical vortex tube. On the other hand, the persistence of core pair vorticity in the multicell intensity was analyzed and it was discovered that the updraft and divergence more influence the persistency of core vorticity. The core vorticity assumed will be continuously persisted in the multicell formation because we did not know when the vorticity will be zero values. Further analysis is necessary to identify the significance of core vorticity intensity until the dissipating of multicell.

Acknowledgements

The authors express their sincere gratitude to Dr. S. Shimizu from the National Research Institute for Earth Science and Disaster Resilience (NIED), Tsukuba, Japan for the thoughtful discussions and for providing useful suggestions with the software developed regarding Dual Doppler radar analysis. This work was supported by JSPS KAKENHI Grant Numbers 15H05765, 20H02258. Fauziana Ahmad acknowledges the award of Malaysian Public Service Department Training (HLP) scholarship allowing the research to be undertaken.

References

Ahmad., et al., (2020): Investigation of Single Cell to Multicell in the Cluster Thunderstorms using Vorticity Analysis, Journal of Japan Society of Civil Engineers, Vol. 76, pp. 187-192.

Bluestein, H.B., et al., (1985): Formation of Mesoscale Lines of Precipitation: Severe Squall Lines in Oklahoma during the Spring, J. Atmos. Sci, Vol. 42, pp. 1711-1732.

Browning, et al., (1976): Structure of an Evolving Hailstorm, Part V: Synthesis and Implications for Hail Growth and Hail Suppression, Monthly Weather Review, Vol.104, pp.603-610.

Min-Jang., et al., (2014): Radar reflectivity and wind fields analysis by using two X-band Doppler radar at Okinawa, Japan from 11 to 12 June 2007, Meteorol.Appl.21, pp. 898-909.

Markowski Paul and Hannon Christina (2006): Multiple-Doppler Radar Observations of the Evolution of Vorticity Extrema in a Convective Boundary Layer, Mon. Wea. Rev, Vol. 134, pp. 355-374.

Markowski Paul and Richardson Yvette (2010): Mesoscale Meteorology in Midlatitudes, John Wiley & Sons, Ltd, ISBN: 978-0-470-74213-6.

Nakakita, E., et al., (2017): Early Identification of Baby-Rain-Cell Aloft in a Severe Storm and Risk Projection for Urban Flash Flood, Advances in Meteorology, Vol. 2017, pp. 1-15.

Ohno, H. and Takemi, T. (2010): Mechanisms for Intensification and Maintenance of Numerically Simulated Dust Devils, Atmosph. Sci. Lett., 11, pp. 27-32.

Protat Alain and Zawadzki Isztar (1999): A Variational Method for Real-Time Retrieval of Three-Dimensional Wind Field from Multiple-Doppler Bistatic Radar Network Data, J. Atmos. Oceanic Technol., Vol. 16, pp. 432-449.

Ronald E. Rinehart (2004): Radar for Meteorologists, Rinehart Publication, ISBN: 0-9658002-1-0.

Shimizu Shingo., et al., (2008): Structure and Formation Mechanism on the 24 May 2000 Supercell-Like Storm Developing in a Moist Environment over the Kanto Plain, Japan, Monthly Weather Review, Vol. 136, pp. 2389-2407.

(Received August 31, 2021)